Title

HCLK2 is essential for the mammalian S-phase checkpoint and impacts on Chk1 stability

Journal

Nature Cell Biology, 9(4)

ISSN

1465-7392

Authors

Collis, Spencer J
Barber, Louise J
Clark, Allison J
et al.

Publication Date

2007-04-01

DOI

10.1038/ncb1555

Peer reviewed

nature cell biology

HCLK2 is essential for the mammalian S-phase checkpoint and impacts on Chk1 stability

Spencer J. Collis[1], Louise J. Barber[1], Allison J. Clark[1], Julie S. Martin[1], Jordan D. Ward[1] and Simon J. Boulton[1,2]

Here, we show that the human homologue of the *Caenorhabditis elegans* biological clock protein CLK-2 (HCLK2) associates with the S-phase checkpoint components ATR, ATRIP, claspin and Chk1. Consistent with a critical role in the S-phase checkpoint, HCLK2-depleted cells accumulate spontaneous DNA damage in S-phase, exhibit radio-resistant DNA synthesis, are impaired for damage-induced monoubiquitination of FANCD2 and fail to recruit FANCD2 and Rad51 (critical components of the Fanconi anaemia and homologous recombination pathways, respectively) to sites of replication stress. Although Thr 68 phosphorylation of the checkpoint effector kinase Chk2 remains intact in the absence of HCLK2, claspin phosphorylation and degradation of the checkpoint phosphatase Cdc25A are compromised following replication stress as a result of accelerated Chk1 degradation. ATR phosphorylation is known to both activate Chk1 and target it for proteolytic degradation, and depleting ATR or mutation of Chk1 at Ser 345 restored Chk1 protein levels in HCLK2-depleted cells. We conclude that HCLK2 promotes activation of the S-phase checkpoint and downstream repair responses by preventing unscheduled Chk1 degradation by the proteasome.

The DNA damage response (DDR) is a complex process involving the orchestration of highly specialized cell-cycle checkpoints that need to be rapidly activated following the detection of damaged DNA. Each of these signalling cascades involves several unique and overlapping factors — classified as sensors, mediators, transducers and effectors — that ultimately lead to the spatio-temporal assembly of multi-protein complexes at the site of damage[1,2]. The functional importance of checkpoints in maintaining genome stability is highlighted by their conservation throughout eukaryotes. As such, defective checkpoint pathways in human cells leads to the accumulation of aberrant DNA and an increased risk of cancer progression, evident from the many human disease syndromes that result from defects in checkpoint factors[3,4]. Therefore, it is important to understand these complex mechanisms at the molecular level to further our knowledge of cancer progression and treatment.

Checkpoints operate at the G1–S, S and G2–M boundaries of the cell cycle and are controlled by the ATM–Chk2 and ATR–Chk1 pathways. The S-phase checkpoint, which is under the control of the ATR–Chk1 pathway, has an essential role in maintaining replication-fork integrity during normal S-phase by preventing the collapse of stalled replication forks. The S-phase checkpoint also coordinates cell-cycle arrest and subsequent DNA-repair events when the replication fork encounters DNA damage[5,3,6]. Activation and recruitment of the Fanconi anaemia and homologous recombination-repair pathways to sites of replication stress requires an intact S-phase checkpoint[7].

Recent work in mouse models has highlighted a surprising, yet highly important link between biological clock proteins and the DDR[8,9]. It has been shown that two clock proteins, Per1 and Prd4, have integral roles in the ATM–Chk2 DDR pathway[10,11]. Here, we show that HCLK2, an uncharacterized orphan mammalian protein with weak similarity to the *C. elegans* biological clock protein CLK-2, interacts with components of the S-phase checkpoint and has a critical role in this checkpoint and the subsequent activation of both Fanconi anaemia and homologous-recombination repair responses.

RESULTS

HCLK2 interacts with components of the S-phase checkpoint

Studies of *C. elegans clk-2* mutants suggest that CLK-2 has an undetermined role in checkpoint responses to genotoxic stress[12,13]. A putative homologue of CLK-2 from the human genome (HCLK2; KIAA068) possesses weak homology to the *C. elegans* protein within a central core of 550 amino acids (Fig. 1a). Polyclonal antibodies that specifically recognise endogenous and transfected HA–Flag–HCLK2, and are capable of immunoprecipitating HCLK2 from cell extracts, were developed to investigate HCLK2 function (Fig. 1b). The band detected by western blotting is depleted using *HCLK2* small interfering RNAs (siRNAs; Fig. 1b).

A combination of mass spectrometry and western blotting identified the checkpoint kinase ATR as a factor that immunoaffinity copurifies with endogenous HCLK2 from HeLa extracts (Fig. 1c). The association of HCLK2 and ATR was confirmed with two independently derived HCLK2 antibodies (Fig. 1d and see Supplementary Information,

[1]DNA Damage Response Laboratory, Cancer Research UK, The London Research Institute, Clare Hall Laboratories, South Mimms, EN6 3LD, UK
[2]Correspondence should be addressed to S.J.B. (e-mail: simon.boulton@cancer.org.uk)

Received 28 November 2006; accepted 23 February 2007; published online 25 March 2007; DOI: 10.1038/ncb1555

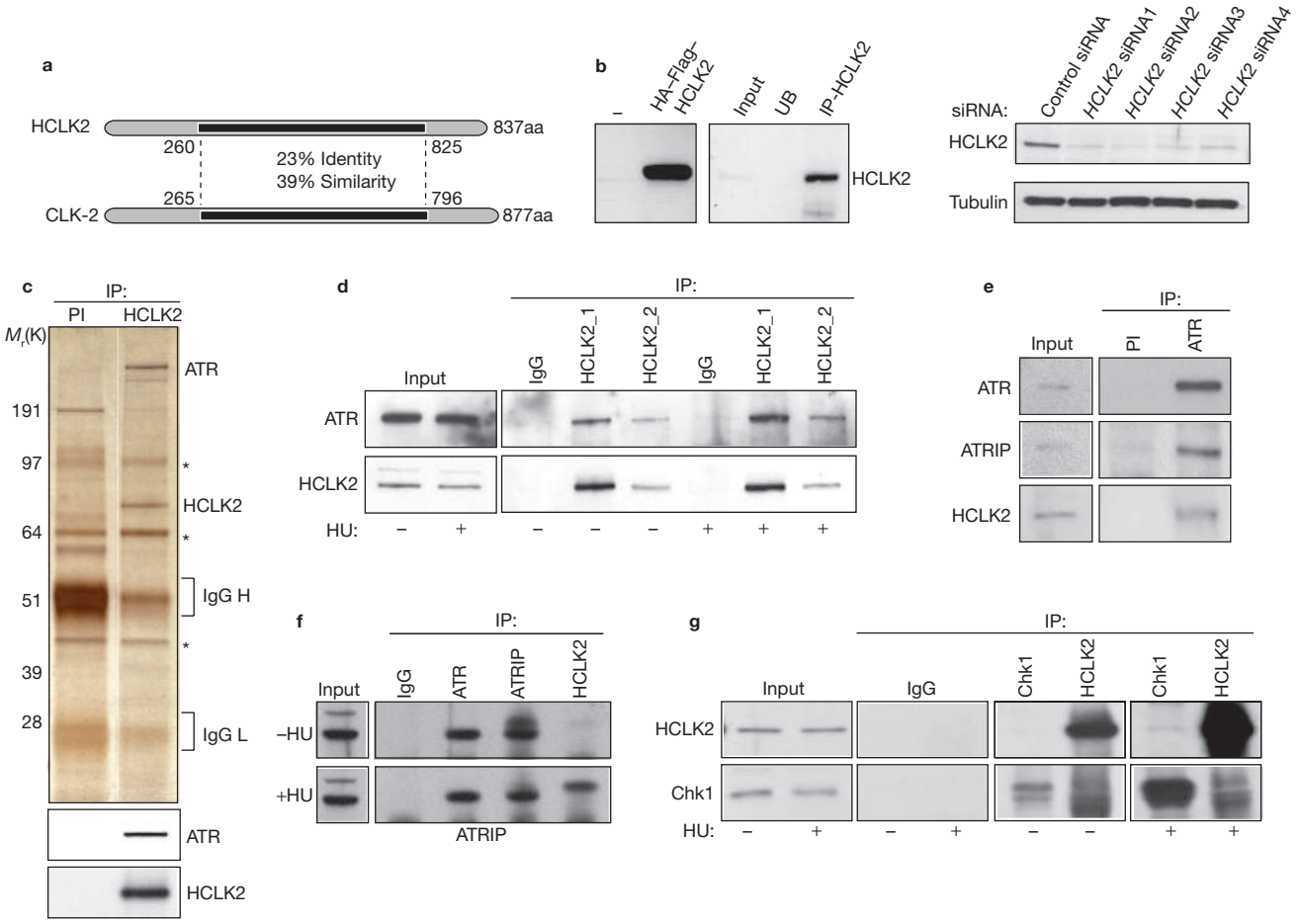

Figure 1 HCLK2 interacts with components of the S-phase checkpoint. (**a**) A schematic representation of human HCLK2 (KIAA0683) and *C. elegans* CLK-2 proteins showing identity and similarity over the central core (black). (**b**) Western blotting with HCLK2 antibodies against endogenous HCLK2 (–), transfected HA–Flag–HCLK2, immunoprecipitated HCLK2 (IP-HCLK2) with corresponding input and unbound fractions, and after transfection of either control or four different *HCLK2* siRNAs. (**c**) Mock/preimmune (PI) and HCLK2 immunoprecipitated proteins from HeLa cells, resolved on a 4–12% gradient SDS–PAGE gel and silver stained. ATR and HCLK2 are shown. Non-specific bands are marked with asterisks and heavy and light IgG bands are indicated. The lower panels show western blots for ATR and HCLK2 from the same immunoprecipitated samples. (**d**) Western blotting for ATR and HCLK2 following immunoprecipitation for HCLK2 from untreated or hydroxyurea (3 mM, 2 h)-treated HeLa-cell extracts with two independently derived HCLK2 antibodies (anti-HCLK2_1 and anti-HCLK2_2). (**e**) Western blotting for ATR, ATRIP and HCLK2 after immunoprecipitation with pre-immune (PI) or ATR antibodies from untreated HeLa cell extracts. (**f**) Western blotting for ATRIP after immunoprecipitation for ATR, ATRIP or HCLK2 from untreated or hydroxyurea (3 mM, 2 h)-treated HeLa-cell extracts. (**g**) Western blotting for HCLK2 and Chk1 after immunoprecipitation for HCLK2 and Chk1 from untreated or hydroxyurea (3 mM, 2 h)-treated HeLa-cell extracts. HU, hydroxyurea.

Fig. S1a). HCLK2 and ATRIP, a known ATR interacting partner[5], coimmunoprecipitated with ATR antibodies (Fig. 1e). Reciprocal coimmunoprecipitation of HCLK2 and ATRIP was also detected (Fig. 1f and see Supplementary Information, Fig. S1b). Furthermore, a weak but reproducible interaction between HCLK2, claspin and Chk1 was observed that was enhanced with hydroxyurea treatment (Fig. 1g and see Supplementary Information, Fig. S1c). Although HCLK2 and Chk1 reciprocally coimmunoprecipitated, HCLK2 was not reproducibly detected in claspin immunoprecitates, which could be due to epitope masking (Fig. 1g and see Supplementary Information, Fig. S1c). Interactions between HCLK2 and the 9-1-1 complex or with the homologous-recombination factor Rad51 were not observed under any conditions tested (data not shown). These results raise the possibility that HCLK2 directly functions in the S-phase checkpoint, analogous to its *C. elegans* counterpart[12,13].

HCLK2 prevents spontaneous DNA damage and is required for intra-S-phase arrest after DNA damage

The S-phase checkpoint has a critical role in preventing spontaneous replication-fork collapse during unperturbed S-phase[14]. After *ATR* or *HCLK2* depletion (Fig. 2a), approximately 35% of cells exhibit extensive focus formation of the ssDNA-binding protein sub-unit RPA32 under non-challenged conditions, compared with 5% of cells with control siRNA (Fig. 2b, c). Furthermore, ubiquitination events mediated by the breast cancer tumour suppressor protein BRCA1, triggered by single-strand DNA (ssDNA) accumulation in S-phase[15], are also induced in 15% of *HCLK2*-depleted cells compared with 2% of cells with control siRNA (Fig. 2b, c and see Supplementary Information, Fig. S2c). In contrast, ATR depletion compromises this response, as previously shown[15]. (Note, blocking S-phase entry with roscovitine or aphidicolin in the absence of HCLK2 reduces the number of cells with

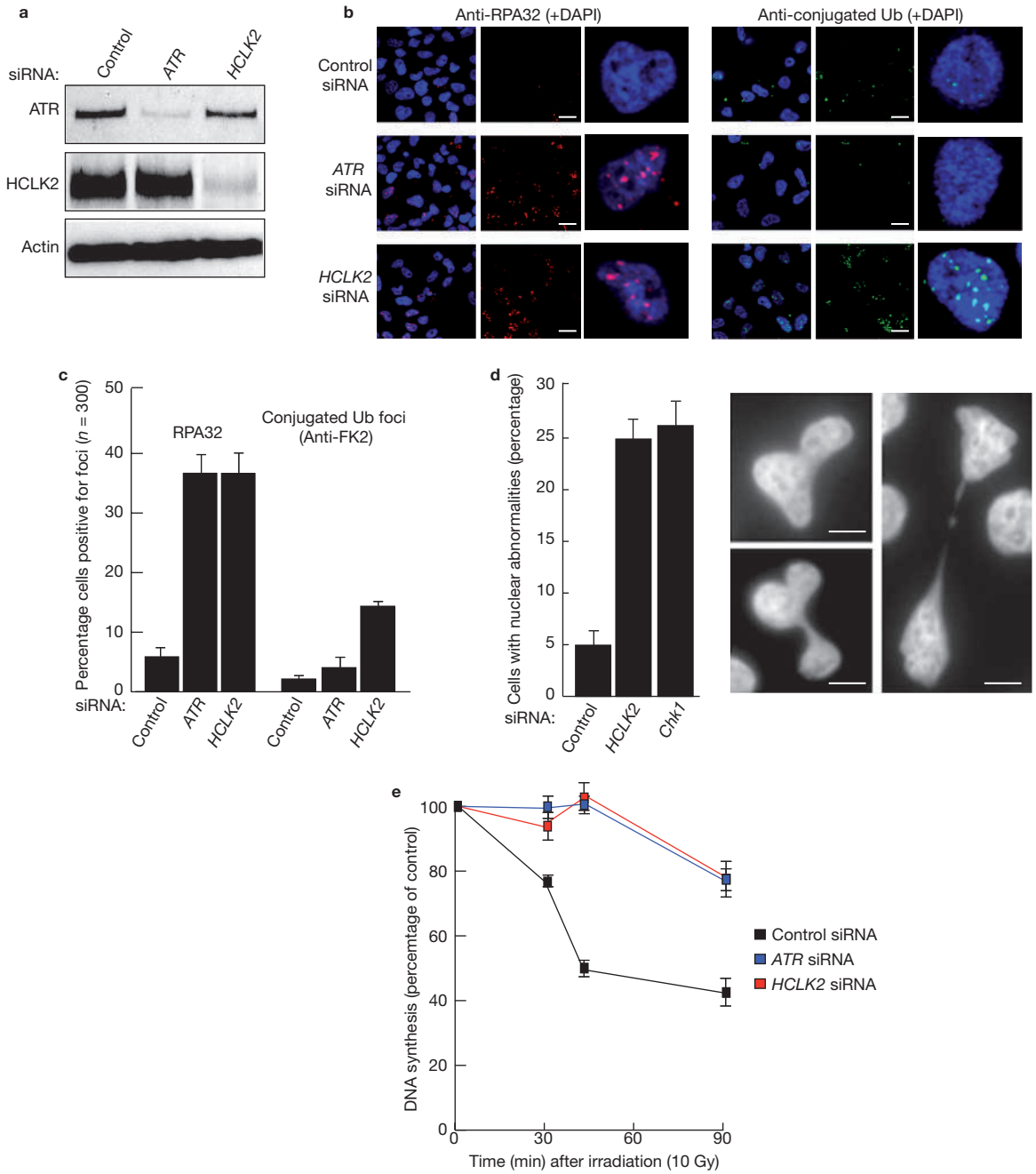

Figure 2 *HCLK2*-deficient cells exhibit S-phase checkpoint defects. (**a**) Western blotting for ATR, HCLK2 and actin from HeLa cells 48 h after siRNA transfection with control, *ATR* and *HCLK2* siRNAs. (**b**) Representative images of RPA32 and conjugated ubiquitin (Ub; FK2) immunostaining in untreated HeLa cells after transfection of control, *ATR* or *HCLK2* siRNAs. Merge of antibody and DAPI staining is shown in the left panels. Antibody staining alone is shown in the middle panels. The far right panel shows a representative magnified image of a single nucleus stained with the indicated antibody and merged with DAPI (the box is 10 μm in diameter). (**c**) Quantification of the number of cells positive for either RPA32 or conjugated ubiquitin foci after transfection of control, *ATR* and *HCLK2* siRNAs. The error bars indicate mean ± s.e.m. from three independent experiments. **(d)** HeLa cells were transfected with control, *HCLK2* or *Chk1* siRNAs. Cells were fixed, stained with DAPI and the percentage of cells with aberrant nuclear morphology (representative images are shown) was measured in a total of 400 cells per genotype. The results obtained are the average of three independent experiments and the error bars represent s.e.m. **(e)** Radio-resistant DNA synthesis assay in control, *ATR* and *HCLK2*-depleted cells irradiated with 10 Gy and allowed to recover for 30, 45 and 90 min. The error bars represent s.e.m. from three independent experiments. The scale bars represent 10 μm in **b** and 5 μm in **d**.

spontaneous DNA damage; see Supplementary Information, Fig. S2). Furthermore, γH2AX and ATR foci are also elevated in the absence of HCLK2 (see Supplementary Information, Fig. S2a, b). Previous studies have shown that deficiency in the topoisomerase II binding protein, TopBP1, leads to aberrant mitosis[17]. Indeed, depletion of HCLK2 or Chk1 resulted in a pronounced increase in abnormal mitoses (Fig. 2d). These data suggest that HCLK2 facilitates replication-fork progression and prevents the accumulation of DNA damage during normal S-phase[16–18].

The S-phase checkpoint is also responsible for inhibiting S-phase progression after DNA damage. Radio-resistant DNA synthesis (RDS) is a hallmark of S-phase checkpoint deficiency and can be measured by

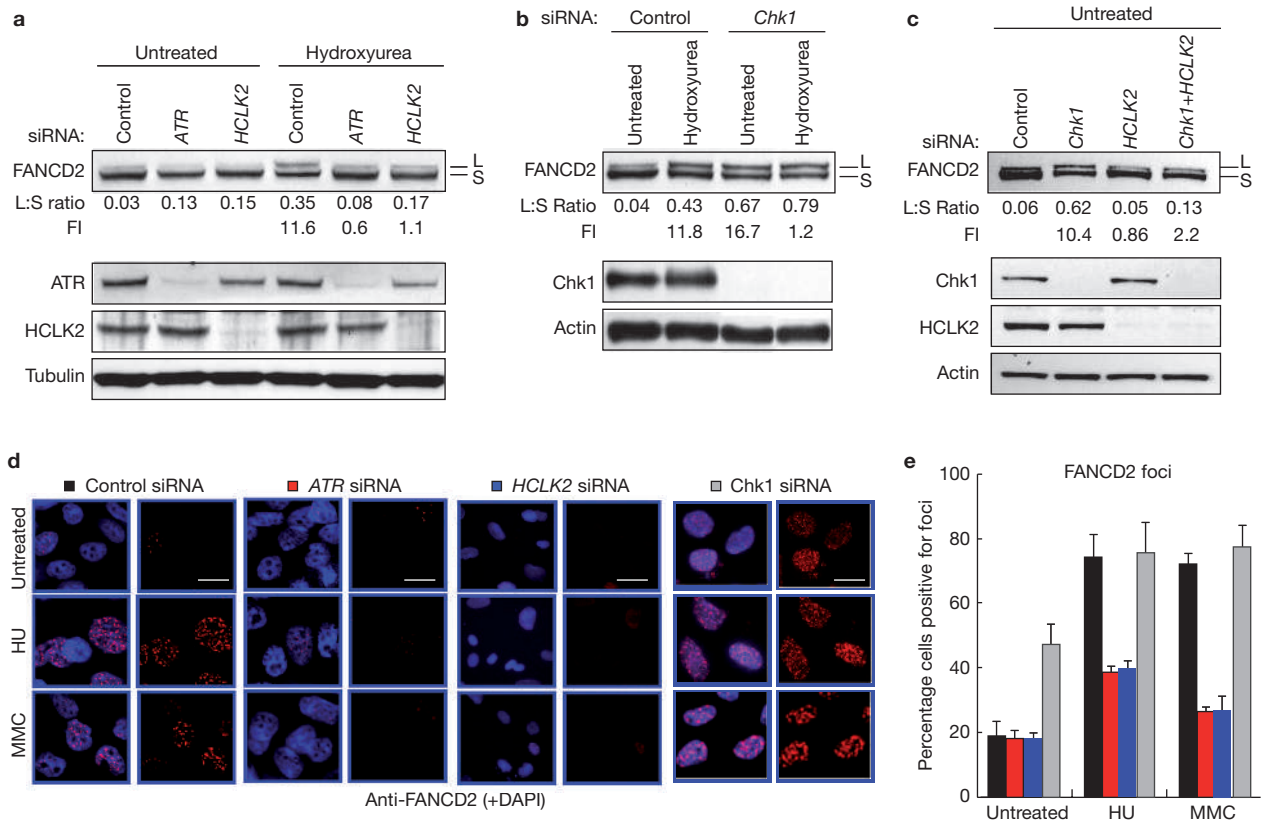

Figure 3 HCLK2 is required for damage-induced FANCD2 monoubiquitination and recruitment to sites of replication stress. (**a**) Western blotting for FANCD2, ATR, HCLK2 and tubulin after transfection with control, *ATR* and *HCLK2* siRNA, in untreated and 3 mM hydroxyurea (2 h)-treated HeLa cells. The levels of S (non-ubiquitinated) and L (monoubiquitinated) isoforms of FANCD2 were quantified using Biorad geldoc quantity-one software and are expressed as the L:S ratio. Fold induction (FI) is L:S ratio of hydroxyurea treated:untreated. (**b**) Untreated and 3 mM hydroxyurea-treated cells transfected with control and *Chk1* siRNA, and examined by western blotting for FANCD2, Chk1 and actin. FANCD2 L:S ratio and fold induction as in **a**. (**c**) Untreated HeLa cells transfected with control, *Chk1*, *HCLK2* or *Chk1* + *HCLK2* siRNAs were examined by western blotting for FANCD2, Chk1, HCLK2 and actin. FANCD2 L:S ratio and fold induction as in **a**. (**d**) Representative images of untreated, 3 mM hydroxyurea-treated and 80 ng ml^{-1} MMC-treated HeLa cells transfected with the indicated siRNA, immunostained with antibodies specific to FANCD2 and counter-stained with DAPI. Merge of antibody and DAPI is shown in the left panels and antibody staining alone is shown in the right panels. The scale bars represent 10 μm. (**e**) Quantification of FANCD2 focus formation. The number of nuclei positive for FANCD2 foci was measured in 150 cells for each siRNA. The error bars indicate the s.e.m. from three independent experiments. Control siRNA, black bars; *HCLK2* siRNA, blue bars; *ATR* siRNA, red bars; *Chk1* siRNA, grey bars.

incorporation of tritiated thymidine before and in response to DNA damage[19]. Control siRNA-treated cells exhibited a decrease of approximately 60% in the rate of DNA synthesis in response to irradiation-induced DNA damage (Fig. 2e). In contrast, cells treated with *HCLK2* or *ATR* siRNA displayed an RDS phenotype with less than 20% reduction in the rate of DNA synthesis after irradiation (Fig. 2e). Thus, HCLK2 is required to efficiently inhibit replication-fork progression in response to DNA damage[20–28].

HCLK2 is required for activation of the Fanconi anaemia pathway after replication stress

It is known that the S-phase checkpoint facilitates damage-induced monoubiquitination of FANCD2 and recruitment to sites of replication stress[29,30]. In untreated control, *ATR* or *HCLK2* siRNA cells, FANCD2 was present mainly in a nonubiquitinated form (FANCD2-S; Fig. 3a). After hdroxyurea or Mitomycin C (MMC) treatment, cells transfected with control siRNA exhibited damage-induced FANCD2 monoubiquitination as revealed by the increase in the level of the FANCD2-L isoform relative to FANCD2-S (Fig. 3a). In contrast, hydroxyurea treatment of cells transfected with *ATR* or *HCLK2* siRNA failed to significantly induce FANCD2 monoubiquitination (Fig. 3a and see Supplementary Information, Fig. S1d). Surprisingly, depletion of *Chk1* led to a tenfold elevation in the basal level of the FANCD2-L isoform in untreated cells, relative to the control (Fig. 3b). Following hydroxyurea treatment, the levels of the FANCD2-L isoform were not further induced in the absence of Chk1 (ref. 31). HCLK2 seems to function upstream of Chk1, as simultaneous depletion of *HCLK2* and *Chk1* resulted in a fivefold reduction in the levels of the FANCD2-L isoform relative to the levels observed in cells depleted for *Chk1* alone (Fig. 3c).

Monoubiquitination is known to target FANCD2 to repair foci[32]. Cells transfected with control, *ATR* or *HCLK2* siRNA display a similar basal level (20%) of untreated cells containing FANCD2 foci. In contrast, approximately 50% of untreated cells treated with *Chk1* siRNA displayed FANCD2 foci (Fig. 3d, e), consistent with the high basal levels of FANCD2 monoubiquitination (Fig. 3b). In control siRNA cells, hydroxyurea or MMC treatment resulted in a dramatic induction in FANCD2 focus formation 18 h after treatment (Fig. 3d, e). However, *HCLK2* or *ATR* siRNA compromised both hydroxyurea- and MMC-induced FANCD2 focus formation (Fig. 3d, e). Importantly, cell-cycle analysis indicated that the defect in damage-induced

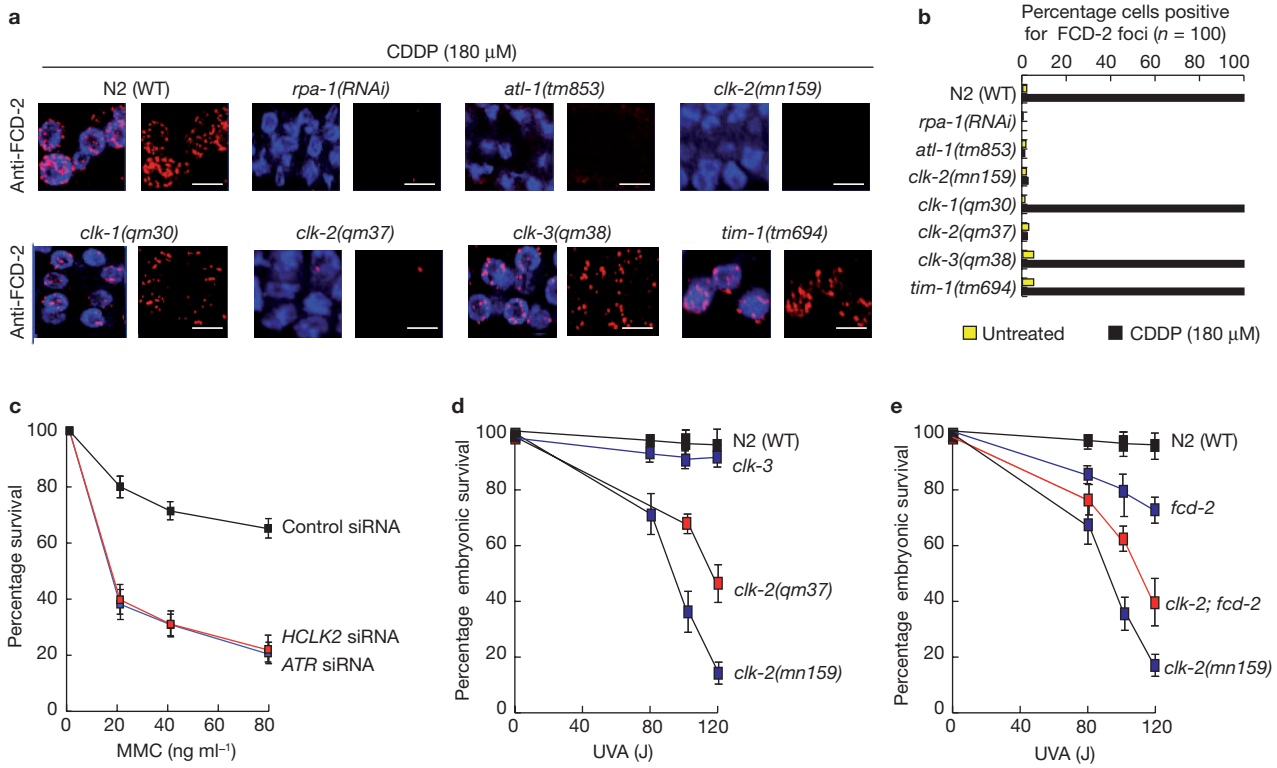

Figure 4 *C. elegans clk-2* mutants and *HCLK2*-deficient human cells exhibit similar defects in FANCD2 function and ICL repair. (**a**) Representative images of FCD-2 immunostaining[33] in the mitotic region of the germline 18 h after treatment with 180 μM cisplatin (CDDP) in animals of the indicated genotype. Animals were grown and treated at 25 °C, the non-permissive temperature for *clk-2(mn159)* and *clk-2(qm37)* strains. A defect in FCD-2 focus formation in *rpa-1(RNAi), atl-1(tm853), clk-2(mn159)* and *clk-2(qm37)* was also observed after treatment with 40 mM hydroxyurea (data not shown). FCD-2 focus formation remains intact in *clk-1(qm30), clk-3(qm38)* and *tim-1(tm694)* mutants. Merge of antibody and DAPI is shown in the left panels and antibody staining alone is shown in the right panels. The scale bars represent 5 μm. (**b**) Quantification of the number of cells in the mitotic region of the germline positive for RPA-1, ATL-1 or FCD-2 foci before (yellow bars) and 18 h after treatment with 180 μM CDDP (black bars) in animals of the indicated genotype. The error bars represent s.e.m. from 100 nuclei. (**c**) Sensitivity of control (black), *HCLK2* (blue) and *ATR* (red) siRNA-depleted HeLa cells to MMC (16 h). The error bars represent s.e.m. from three independent experiments. (**d**, **e**) Percentage progeny survival from worms of the indicated genotype before and after treatment with 10 μg ml^{-1} trimethylpsoralen (TMP) plus UVA in the range indicated. Strains were grown at 20 °C. The error bars represent mean ± s.e.m. (n = 24).

activation of FANCD2 in the absence of ATR or HCLK2 was not due to the accumulation of cells at a cell-cycle stage incompatible with FANCD2 monoubiquitination or focus formation (see Supplementary Information, Fig. S3). Thus, HCLK2 is required for efficient damage-induced monoubiquitination and focus formation of FANCD2, similar to that previously reported for RPA, ATR and Nijmegen breakage syndrome (Nbs1)-deficient cells[29,30].

To determine whether the role of HCLK2 in Fanconi anaemia-pathway activation is conserved, the contribution of *clk-2* in the recruitment of the *C. elegans* homologue of FANCD2 (FCD-2)[33] to sites of replication stress was assessed. Two independently derived temperature-sensitive alleles of *clk-2* (*mn159* and *qm37*) remained intact for cisplatin and hydroxyurea-induced FCD-2 focus formation at the permissive temperature (15 °C; see Supplementary Information, Fig. S4b). In contrast, cisplatin and hydroxyurea-induced FCD-2 focus formation was abolished in *clk-2* mutants shifted to the non-permissive temperature (25 °C; Fig. 4a, b and see Supplementary Information, Fig. S4b), and was also compromised in *atl-1* (ATR) mutants and in animals subjected to *rpa-1* RNA interference (RNAi), consistent with recent data from mammalian cells[29,30]. However, *clk-1*, *clk-3* or *tim-1* mutants that encode biological clock proteins and the Timeless protein, respectively, displayed wild-type levels of FCD-2 foci following replication stress (Fig. 4a, b). These data reveal a conserved role for RPA-1, ATL-1 and CLK-2 in promoting FCD-2 focus formation in response to replication stress — a role not shared by all biological clock proteins.

It is known that cells deficient for FANCD2 monoubiquitination and assembly into repair foci are rendered sensitive to interstrand crosslink (ICL)-inducing agents[7,33]. Indeed, cells depleted for *HCLK2* or *ATR* were hypersensitive to the cytotoxic effects of MMC when compared with control cells (Fig. 4c). Moreover, *C. elegans clk-2* mutants also exhibited sensitivity to ICL-inducing agents, whereas *clk-3* mutants displayed wild-type sensitivity (Fig. 4d). Interestingly, *clk-2; fcd-2* double mutants did not exhibit synergistic sensitivity to ICL-inducing agents, indicating that *clk-2* and *fcd-2* function in a common repair pathway (Fig. 4e). Taken together, these data indicate that HCLK2 and its *C. elegans* counterpart have a conserved role in facilitating ICL repair.

HCLK2 regulates homologous-recombination repair after replication stress

It has been shown that Chk1 activation is required for homologous-recombination repair at sites of replication stress[34], but it is unclear whether this function is also shared by other components of the S-phase checkpoint. Rad51 foci were present at low levels in a subset

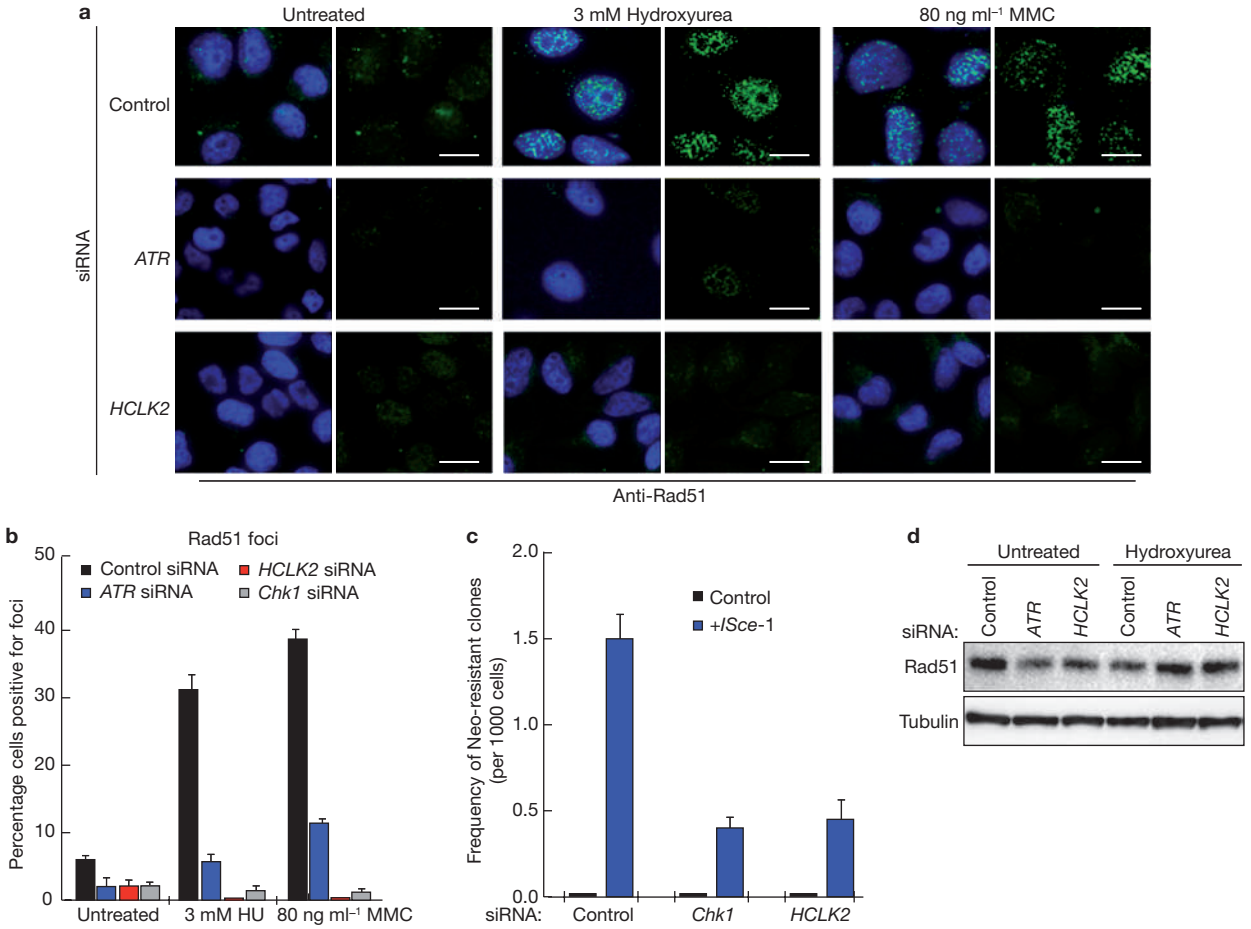

Figure 5 HCLK2 is required for homologous-recombination repair following replication stress. (**a**) Representative images of fixed HeLa cells transfected with the indicated siRNAs, and immunostained for Rad51 with DAPI counter-staining. Cells were either untreated, or treated with 3 mM hydroxyurea (2 h) or 80 ng ml^{-1} MMC (16 h). Merge of antibody and DAPI is shown in the left panels and antibody staining alone is shown in the right panels. The scale bars represent 10 μm. (**b**) Quantification of Rad51 focus formation for untreated, 3 mM hydroxyurea (2 h) or 80 ng ml^{-1} MMC-treated HeLa cells. Cells were transfected with control (black bars), *ATR* (blue bars), *HCLK2* (red bars) and *Chk1* (grey bars) siRNA. The error bars represent s.e.m. from three independent experiments. (**c**) Analysis of the frequency of I*Sce*-1-induced homologous recombination using a neomycin-based reporter construct in control, *Chk1* and *HCLK2* siRNA-transfected SW480sn3 cells. The error bars represent s.e.m. from three independent experiments and *P* values are less than 0.05 for both *HCLK2* and *Chk1* siRNAs compared to control. Similar defects are also observed using an alternative GFP-based homologous-recombination reporter (data not shown)[17]. (**d**) Western blotting for Rad51 and tubulin in extracts prepared from untreated and 3 mM hydroxyurea-treated cells transfected with control, *ATR* and *HCLK2* siRNAs.

of untreated control, *ATR*, *HCLK2* and *Chk1* siRNA cells (Fig. 5a, b). After hydroxyurea or MMC treatment, Rad51 foci were induced in control siRNA cells, with 31.4% and 39.2% of cells within the population showing extensive Rad51 focus formation, respectively (Fig. 5a, b). However, hydroxyurea and MMC treatment failed to induce Rad51 foci after treatment with *ATR*, *HCLK2* or *Chk1* siRNA (Fig. 5a, b), which was not due to decreased Rad51 protein levels in *ATR* or *HCLK2*-depleted cells (Fig. 5d). We also used a homologous recomination-reporter assay in SW480sn3 cells that measures homologous-recombination frequencies in an integrated neomycin plasmid[34–37]. *HCLK2* or *Chk1* siRNA-depleted SW480sn3 cells produced *neo* resistant (*neo*^{R}) recombinants at a frequency greater than fourfold lower than the control siRNA-treated cells (Fig. 5c). Furthermore, simultaneous siRNA depletion of *HCLK2* and *Chk1* did not confer an additive homologous-recombination defect, as the frequency of homologous-recombination events was equivalent to that observed in cells depleted for either *HCLK2* or *Chk1* alone (data not shown). Taken together, these data suggest that HCLK2 and Chk1 function in the same pathway to promote Rad51 recruitment and homologous recombination-mediated repair in response to replication stress.

Chk1 instability compromises claspin phosphorylation and Cdc25A degradation in the absence of HCLK2

To examine the cause of the checkpoint defect in *HCLK2*-depleted cells, we assessed the integrity of responses downstream of ATR recruitment, including Chk1 Ser 345 phosphorylation, Chk2 Thr 68 phosphorylation, claspin phosphorylation and Cdc25A degradation[26,37,38]. No detectable Chk1 phosphorylation at Ser 345 was observed in untreated control, *ATR* or *HCLK2* siRNA cells (Fig. 6a). However, control cells treated with hydroxyurea exhibited robust Chk1 phosphorylation at Ser 345 (Fig. 6a). In contrast, Chk1 phosphorylation at Ser 345 was markedly reduced in *ATR* or *HCLK2*-depleted cells after hydroxyurea treatment, which in the case of HCLK2, was not due to a defect in phosphorylation, but was caused by an overall reduction in total Chk1 protein

levels (Fig. 6a). The mobility shift induced by claspin phosphorylation observed in control siRNA treated cells was also compromised following *ATR* or *HCLK2* siRNA (Fig. 6a)[39–41]. Furthermore, Cdc25A, which controls mitotic entry and is targeted for degradation in control cells in response to replication stress by Chk1-mediated phosphorylation[3], was not efficiently degraded after hydroxyurea-treatment in cells treated with *HCLK2* siRNA (Fig. 6b). However, Chk2 Thr 68 phosphorylation in response to hydroxyurea-treatment remained intact in control, *ATR* and *HCLK2* siRNA (Fig. 6c). Taken together, these data indicate that HCLK2 is required for claspin phosphorylation and Cdc25A degradation in response to replication stress.

It was noted that the total Chk1 protein levels in *HCLK2*-depleted cells varied between experiments, with levels ranging from 40–80% of those observed in control cells (Fig. 6a and see Supplementary Information, Fig. S1d–f). This is likely because of fluctuations in the levels of spontaneous replication stress within asynchronous cell-culture populations treated with *HCLK2* siRNA (Fig. 2). Importantly, this phenotype was observed with two individual *HCLK2* siRNAs (see Supplementary Information, Fig. S1d), and was not caused by an off-target effect of *HCLK2* siRNA on *Chk1* mRNA as similar transcript levels were present in control and *HCLK2* siRNA cells before and after hydroxyurea treatment (Fig. 7a). Similarly to endogenous Chk1, depletion of *HCLK2* also significantly reduced the levels of transfected Flag–Chk1 relative to controls (Fig. 7b). It has been previously shown that Chk1 is subjected to proteasome-dependent degradation following replication stress[42]. Time-course analyses revealed that the overall rate of Chk1-protein degradation between 0 and 8 h after hydroxyurea treatment was increased 2.8 ± 0.6-fold ($P = 0.002$; calculated from three independent experiments) in *HCLK2*-depleted cells relative to control cells. At early time points after hydroxyurea-treatment (0 and 2 h) the rate of Chk1 degradation was increased 4.5 ± 0.5-fold in the absence of *HCLK2* (Fig. 7c and see Supplementary Information, Fig. S1e).

As it has been shown that ATR-mediated phosphorylation of Chk1 at Ser 345, but not at Ser 317, targets Chk1 for proteasome dependent degradation[42], we assessed the impact of inactivation of ATR, or mutation of Chk1 at Ser 317 or Ser 345, on the levels of Chk1 present in *HCLK2*-depleted cells. Analogous to wild-type Chk1, levels of transfected Myc–Chk1 mutated at Ser 317 were reduced in *HCLK2*-depleted cells, but not after treatment with control siRNA (Fig. 7d). However, transfected Myc–Chk1 mutated at Ser 345 that is resistant to ubiquitin dependent degradation[42] was not significantly reduced after hydroxyurea treatment in control or *HCLK2* siRNA-treated cells (Fig. 7d). Furthermore, simultaneous depletion of *ATR* and *HCLK2* restored Chk1 to levels approaching those observed in cells treated with control or *ATR* siRNA (Fig. 7e). Collectively, these data suggest that HCLK2 is required for Chk1 stability in unperturbed cells and protects Chk1 from rapid ubiquitin-dependent degradation following the induction of replication stress (Fig. 8).

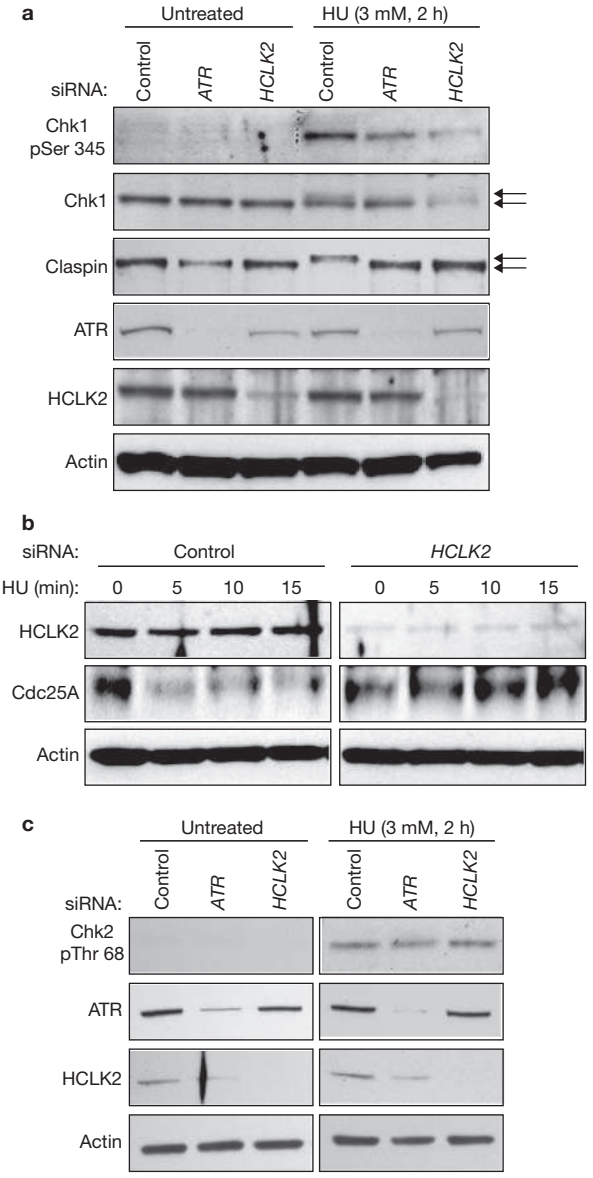

Figure 6 *HCLK2* depletion compromises claspin phosphorylation and Cdc25A degradation in the absence of HCLK2, but not Chk2 pThr 68 phosphorylation. (**a**–**c**) Western blotting with the indicated antibodies of extracts derived from control, *HCLK2* and *ATR* siRNA treated cells before and 2 hours after treatment with 3 mM hydroxyurea. Chk1 pSer 345 and claspin phosphorylation following hydroxyurea-treatment of HeLa cells (**a**). The arrows indicates the band shift resulting from Chk1 and claspin phosphorylation after hydroxyurea treatment. Cdc25A degradation after hydroxyurea-treatment (**b**). Forty-eight hours after siRNA transfection, 3 mM hydroxyurea and 25 μg ml^{-1} cyclohexamide was added to cells and whole-cell extracts were generated at the indicated times after treatment. Western blots of cell lysates probed for the indicated proteins are shown. Chk2 pThr 68 phosphorylation after hydroxyurea-treatment in control, *ATR* and *HLCK2* siRNA-treated Hela cells (**c**).

DISCUSSION

Studies in *C. elegans* have suggested a role for the biological clock protein CLK-2 in checkpoint responses to DNA damage[12,13]. Before this study, it was not known how CLK-2 contributed to the DDR or whether its putative homologues in complex eukaryotes performed a similar function in DDR pathways. Here, we demonstrate that HCLK2 associates with ATR, ATRIP, claspin and Chk1, and is essential for many aspects of the S-phase checkpoint in mammalian cells: first, cells lacking HCLK2 accumulate spontaneous DNA damage in S-phase and exhibit abnormal mitoses analogous to ATR, Chk1 and TopB1-deficient cells[17,43]. This suggests that HCLK2 has an important function in promoting replication fork stability and/or progression, and prevents mitotic entry in the presence of DNA damage. Second,

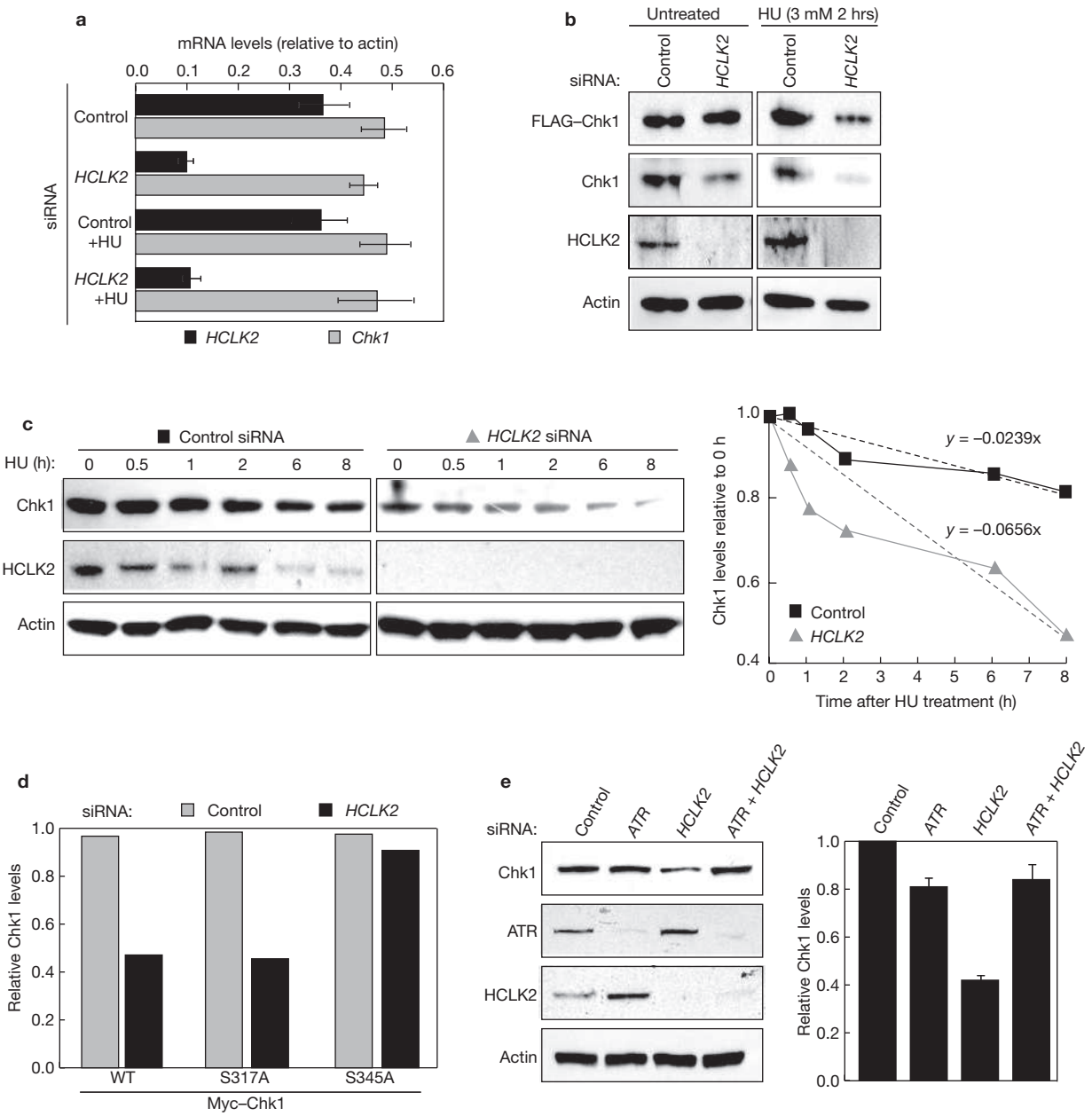

Figure 7 Chk1 instability in *HCLK2*-depleted cells is dependent on ATR phosphorylation of Chk1 at Ser 345. (**a**) *HCLK2* and *Chk1* mRNA levels normalized to *actin* mRNA measured by quantitative RT–PCR in control and *HCLK2* siRNA-treated HeLa cells before and 2 h after treatment with 3 mM hydroxyurea. The error bars represent s.e.m. from three independent experiments. (**b**) Western blotting for transfected Flag–Chk1, endogenous Chk1, HCLK2 and actin after transfection with Flag–Chk1 with control or *HCLK2* siRNA, on untreated and 3 mM hydroxyurea (2 h)-treated HeLa cells. (**c**) Western blotting for Chk1, HCLK2 and actin protein levels in extracts derived from control and *HCLK2* siRNA treated cells at the indicated times (h) after treatment with 3 mM hydroxyurea. The graph shows the levels of Chk1 protein quantified by densitometry using Biorad geldoc quantity-one software and normalized to actin in control and *HCLK2* siRNA treated cells. Values are for each time point and are shown relative to the levels of Chk1 at the 0 h time point (also see Supplementary Information, Fig. S1e). Linear-regression analyses were performed on the resulting data curves to obtain the rate of Chk1 degradation and/or decay: between the 0 and 8 h time points (rate *HCLK2* siRNA/control siRNA = –0.0656/–0.0239 = 2.74-fold); between 0 and 2 h time points (rate *HCLK2* siRNA/control siRNA = –0.1582/–0.0376 = 4.21-fold). The average rate from three independent experiments is 2.8 ± 0.6-fold ($P = 0.002$). The rate of Chk1 degradation after hydroxyurea is slightly increased in *HCLK2*-depleted cells treated with cycloheximide (3.2-fold 0–8 h, relative to control; data not shown). (**d**) Cells were subjected to control or *HCLK2* siRNA and then transfected with wild-type (WT) Myc–Chk1, Myc–Chk1^{S317A} or Myc–Chk^{S345A}. Average Chk1 protein levels quantified from western blots of two independent experiments using Biorad geldoc quantity-one software relative to wild-type Myc–Chk1 levels in control siRNA cells are shown (also see Supplementary Information, Fig. S1f). (**e**) Western blotting for the indicated proteins in extracts derived from control, *ATR*, *HCLK2* and *ATR* + *HCLK2* siRNA-treated HeLa cells. Quantification of Chk1 protein levels from three independent experiments is shown in the graph. The error bars represent s.e.m.

HCLK2-deficient cells exhibit an RDS phenotype indicating that HCLK2 also functions in orchestrating the S-phase checkpoint response after exposure to DNA-damaging agents. Third, HCLK2 is required for damage-induced monoubiquitination and subsequent recruitment of FANCD2 to sites of replication stress, analogous to ATR[29,30]. Failure to activate and recruit FANCD2 in the absence of HCLK2 also confers sensitivity to ICL-inducing agents, a hallmark of Fanconi anaemia-deficient cells. Finally, activation of homologous recomination-mediated repair through Rad51 recruitment to sites of replication stress also requires ATR and HCLK2. This result is consistent with previous studies showing that phosphorylation of Rad51 on Thr 309 by Chk1 is important for activation of homologous recombination-mediated repair after replication stress[34]. Collectively, the failure to stabilize stalled replication forks, to respond to DNA damage in S-phase and to recruit FANCD2 and Rad51 to sites of replication stress indicates that HCLK2 has a critical function in maintenance of genome stability as part of the S-phase checkpoint[44].

Although HCLK2 interacts with ATR–ATRIP, the observation that HCLK2-deficient cells exhibit increased levels of spontaneous RPA32, γH2AX, BRCA1-mediated ubiquitin and ATR foci indicates that HCLK2 is largely dispensable for ATR–ATRIP recruitment and subsequent activation (Fig. 8). Our data indicate that HCLK2 is also dispensable for Chk1 phosphorylation, but is required to maintain Chk1 stability; HCLK2-deficient cells display reduced Chk1 protein levels in unperturbed cells and exhibit an accelerated rate of proteasome-mediated Chk1 degradation when replication stress is further induced after hydroxyurea treatment. Consistent with a recent report that ATR-mediated phosphorylation of Chk1 at Ser 345 not only activates Chk1 but also targets it for ubiquitin dependent degradation[42], we have shown that depletion of ATR or Chk1 mutated at Ser 345 but not at Ser 317 partially restores Chk1 protein levels in HCLK2-depleted cells. This suggests that elevation in response to spontaneous replication stress in HCLK2-depleted cells triggers ATR-dependent phosphorylation of Chk1 at Ser 345 and leads to proteasome-mediated degradation and reduced levels of Chk1. After hydroxyurea treatment, the reduced levels of Chk1 in HCLK2-depleted cells, coupled with an accelerated rate of Chk1 degradation, leads to a reduced capacity to trigger claspin phosphorylation and Cdc25A degradation necessary for efficient S-phase checkpoint activation, and also compromises Rad51 recruitment required to promote homologous recombination-mediated repair (Fig. 8).

Our data also establish that damage-induced activation of the Fanconi anaemia pathway requires both ATR and HCLK2 (Fig. 3), but surprisingly this function is independent of their roles in regulating Chk1 — depletion of Chk1 results in constitutive monoubiquitination and recruitment of FANCD2 to chromatin-associated foci (Fig. 3). The observation that simultaneous depletion of Chk1 and HCLK2 suppresses constitutive Fanconi anaemia-pathway activation implies that HCLK2 functions upstream of Chk1 in regulating this pathway. It is therefore possible that ATR and HCLK2 are required to switch the Fanconi anaemia pathway on in response to replication stress, whereas Chk1 maybe required to downregulate the pathway once DNA integrity is restored. How ATR, HCLK2 and Chk1 control Fanconi anaemia-pathway function remains unclear, yet it is intriguing that the Fanconi anaemia core-complex components FANCA, FANCD2 and FANCM are phosphorylated in response to DNA damage[7].

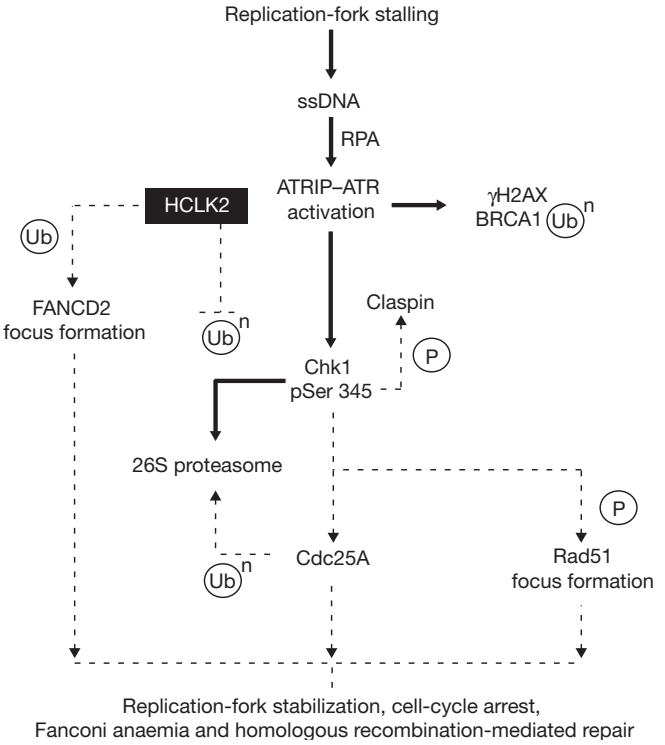

Figure 8 Schematic representation of the role of HCLK2 in regulating the S-phase checkpoint. Thick lines indicate events that are increased in the absence of HCLK2; dotted lines are events that are defective in the absence of HCLK2. P, phosphorylation; Ub, ubiquitination.

Our observation that HCLK2 and Chk1 weakly interact raises the possibility that HCLK2 may directly regulate Chk1 stability. However, it remains to be determined whether this interaction is direct, and as HCLK2 and its homologues lack any known motifs, it is unclear how HCLK2 might perform this function. In future studies it will be important to determine whether HCLK2 binds specifically to Chk1 pSer 345 or ubiquitinated Chk1 pSer 345, and if so, whether this association temporarily prevents access of the E3 ubiquitin ligase for Chk1 or the 26S proteasome. Our data indicate that similarly to Chk1, HCLK2 is a nuclear protein and was not detectably recruited or retained at sites of DNA damage (see Supplementary Information, Fig. S4). Moreover, HCLK2 lacks conserved Ser–Glu motifs that may be targets for ATR phosphorylation. Indeed, no obvious mobility shift of HCLK2 was observed after DNA damage (Fig. 1–7). However, it is intriguing that HCLK2 protein levels noticeably decreased 6–8 h after replication stress, at the time when Chk1 protein levels also began to decrease in control cells (Fig. 7c). It is therefore possible that Chk1 and HCLK2 are coordinately degraded by the proteasome to promote checkpoint termination, but how this is controlled remains unclear.

The observation that HCLK2-depleted cells share many phenotypic abnormalities with cells derived from Fanconi anaemia and Seckel syndrome patients raises the possibility that *HCLK2* may be inactivated in human disease. This may manifest as a hypomorphic mutation similar to ATR mutations associated with Seckel syndrome[45]. Thus, assessing the integrity of the *HCLK2* gene in Fanconi anaemia and Seckel cells that cannot be assigned to known complementation groups will be of great clinical importance. □

METHODS

Cell lines, siRNA and drug treatments. HeLa cells (Cancer Research UK Cell Services, South Mimms, UK) and SW480Sn3 cells (gift from H. Bryant and T. Helleday, Sheffield, UK) were maintained as adherent monolayer cultures in appropriate media at 37 °C in a humidified atmosphere of 5% carbon dioxide. SMARTPool RNAi for *ATR*, *HCLK2* and *Chk1* were purchased from Dharmacon (Lafayette, CO). Individual siRNA sequences are as follows: *ATR*, (sense) GAACAACACUGCAGGUUUGUU, GGUCAGCUGUCUACUGUUAUU, GCAACUCGCCUAACAGAUAUU, ACUGAUGGCUGAUUAUUUAUU and (antisense) 5′PCAAACCAGCAGUGUUGUUCUU, 5′PUAACAGUAGACAGCUGACCUU, 5′PUAUCUGUUAGGCGAGUUGCUU, 5′PUAAAUAAUCAGCCAUCAGUUU; *HCLK2*, (sense) GAGCGGAUCAGAAGCAAGAUU, UGAUGUGCCUGGCUGUUAAUU, GUACGAAGAGGAUGAACUGUU, GAAGACCUGUGUGGUGGGAUU and (antisense) 5′PUCUUGCUUCUGAUCCGCUCUU, 5′PUUAACAGCCAGGCACAUCAUU, 5′PCAGUUCAUCCUCUUCGUACUU, 5′PUCCCACCACACAGGUCUUCUU; *Chk1*, (sense) GCAACAGUAUUUCGGUAUAUU, GGACUUCUCUCCAGUAAACUU, AAAGAUAGAUGGUACAACAUU, CCACAUGUCCUGAUCAUAUUU and (antisense) 5′PUAUACCGAAAUACUGUUGCUU, 5′PGUUUACUGGAGAGAAGUCCUU, 5′PUGUUGUACCAUCUAUCUUUUU, 5′PAUAUGAUCAGGACAUGUGGUU. Sub-confluent monolayers of cells were transfected using 100 nM siRNA with Dharmafect #1 reagent (Dharmacon) in antibiotic-free media. RDS, hydroxyurea (Sigma, Poole, UK) and MMC (Sigma) sensitivity were performed 48 h after siRNA treatment, as previously described[22,30,46,47]. To block entry into S-phase, 10 μg ml^{-1} roscovitine (Sigma) was added to the cells 4 hours before fixation.

Antibodies. The first 400 amino acids of HCLK2 protein were expressed and purified in *Escherichia coli* and used to generate affinity purified rabbit anti-HCLK2 polyclonal antibodies, as previously described[15]. Affinity purified HCLK2 antibodies recognize the same endogenous protein in western blotting as detected with the HCLK2 antibody kindly provided by S. Hekimi (McGill University, Montreal, Canada) and this protein is depleted using four different siRNAs against *HCLK2* (ref. 48). Human primary antibodies used were: HCLK2 (S. Hekimi and as described above); FK2-conjugated ubiquitin (PW8810; Biomol, Exeter, UK); RPA1 and claspin (ab21551 and ab3720; Abcam, Cambridge, UK); ATR (sc1887, Santa Cruz Biotechnology, Santa Cruz, CA; G. Smith, Kudos Pharmaceuticals, Cambridge, UK; and N. Lakin, Oxford University, Oxford, UK); ATRIP (ab19351, Abcam; and S. Jackson, Cambridge University, Cambridge, UK); FANCD2 (NB100-182, Novus Biologicals, Littleton, CO), Chk1 pSer 345 (#2341; Cell Signalling, Danvers, CA), Cdc25a (clone F6, Santa Cruz), Chk1 and tubulin (DCS-310, DM1A, Sigma); actin (ab8226, Abcam); and Rad51 (FBE2, Steve West, South Mimms, UK). Secondary antibodies for immunofluorescence were purchased from Sigma and for western blotting from Dako (Glostrup, Denmark). Human cells were subjected to detergent extraction with Triton X-100 (0.5% for 5 min) to remove the majority of non-chromatin-bound proteins before fixation and immunostaining as previously described[15].

Immunoprecipitation conditions. Approximately 1 × 10^6 monolayered HeLa cells were washed with PBS and lysed on ice in 1 ml buffer containing 20 mM Tris at pH 8.0, 150 mM NaCL, 0.5% NP40, 1 mM EDTA, with protease and phosphatase inhibitor cocktails (P2714 & P5726, Sigma) and 50 U ml^{-1} benzonase (Novagen, Madison, WI) to digest RNA and DNA to eliminate non-specific interactions bridged by DNA and/or RNA. After centrifugation, supernatants were incubated with appropriate antibodies for 1 h before a mixture of protein A and protein G beads were added and the mixture incubated overnight at 4 °C. Beads were then pelleted and washed three times in 20× bed volume of the above buffer (excluding benzonase). Finally, 30 μl 2× SDS sample buffer containing reducing agent was added and the beads were boiled for 5 min. For gel loading, samples were centrifuged to pellet beads and 5 μl of supernatant was added per lane. Inputs represent 1/20th of the extract used for the immunoprecipitation.

Cell-cycle analysis. Treated cells were washed once with PBS, trypsinized, washed again in PBS and then resuspended in 500 μl cell-cycle test Plus buffer (BD Biosciences, Stockholm, Sweden). Cell-cycle distribution was analysed by a FACSCalibur flow cytometer (BD Bioscience) using Cellquest software. ModFit programme was used to analyse the cell-cycle profiles (Verity Software House Inc., Topsham, ME).

Real-time PCR analysis of mRNA levels. siRNA and hydroxyurea treatments were performed on HeLa cells as previously described. RNA preparations were made using the Qiagen RNeasy mini kit, according to the manufacturer's protocol, and subsequently digested with TURBO DNase (Ambion, Austin, TX) following the method for rigorous treatment. Total RNA (1 μg) was converted to cDNA using the Superarray first strand cDNA synthesis kit, according to the manufacturer's protocol. These cDNA samples were then diluted 1:5 for real-time PCR, using the Superarray SYBR green/ROX RT Sigma PCR master mix and RT^2 primer sets for KIAA0683 (*HCLK2*), *CHEK1* and *ACTG1* (actin). Reactions were performed in triplicate using a two-step cycling program (10 min, 95 °C; 40 cycles of 15 s, 95 °C and 1 min, 60 °C; and terminal dissociation protocol) on an ABI Prism 7000 sequence-detection system. Standard curves were produced for each primer set using control cDNA, and all PCR reactions were repeated using appropriately diluted RNA to preclude cellular DNA contamination. Threshold cycle values for each reaction were determined using the ABI Prism software, and converted to a relative expression level according to the straight-line equation obtained from plotting the standard curve threshold cycles against the log template dilution factor. Relative expression levels for each reaction were then normalized to actin levels in the equivalent cDNA sample.

Homologous-recombination assay. Measurement of the frequency of homologous recombination-mediated DSB repair was performed as previously described. Briefly, the assay was performed in SW480sn3 cells that contain a single integrated copy of an *SCneo* substrate[35]. After transfection (48 h) of SW480sn3 cells with control, *HCLK2* or *Chk1* siRNAs, cells were further transfected with an I*Sce*-1 expression plasmid, and were either plated in regular media (500 per dish in triplicate) or in media containing 1 mg ml^{-1} G418 (100,000 per dish in triplicate). After two weeks incubation, the media was removed and colonies stained with Geimsa, washed and counted. The recombination frequency was calculated as follows: the numbers of colonies (containing more than 50 cells) present on non-selected plates was divided by the number plated to give the plating efficiency. This number was multiplied by the number of cells plated on G418-selected plates to give the 'expected' number of colonies. The actual number of colonies present on G418 plates was then divided by the expected number to calculate recombination frequency. Each recombination frequency was multiplied by 1000 to give a number suitable for graphical representation. For all siRNA-treated cells (control, *Chk1*, *HCLK2* and *Chk1–HCLK2*), a replica set of cells were not transfected with the I*Sce*-1 plasmid and equal numbers of cells were then plated in non-G418 and G418-containng media. No colonies grew on any of these dishes indicating that any colonies presented on the I*Sce*-1-tranfected cells were because of recombination of the *G418* gene and not due to background and/or chance recombination events.

Note: Supplementary Information is available on the Nature Cell Biology website.

ACKNOWLEDGEMENTS

We wish to thank: A. Jones and H. Cooper for mass-spectrometry; Y. Murakawa and S. Takeda for laser micro-irradiation experiments; S. Hekimi, S. West, N. Lakin, G. Smith, S. Jackson and A. Jazayeri for HCLK2, Rad51, ATR, ATRIP and Cdc25A antibodies, respectively; N. Mailand, J. Bartek, H. Piwnica-Worms, Y.-W. Zhang and B. Abraham for Chk1 constructs; H. Bryant and T. Helleday for SW480sn3 cells, ISce-1 and GFP-reporter plasmids; N. O'Reilly for peptide synthesis; and R. Peat and R. Horton-Harpin for cell culture. Thanks to J. Svejstrup, P.Zegerman, A. Jazayeri, G. Alderton, J. Falck, P. Robins, M. Segurado and members of the Boulton lab for technical advice and comments on the manuscript. This work was funded by Breast Cancer Campaign (GA3221) and Cancer Research UK.

AUTHOR CONTRIBUTIONS

S.J.C. performed the majority of experiments. L.J.B., A.J.C., J.S.M. and J.D.W. all contributed to the experiments. S.J.B., S.J.C. and L.J.B. contributed intellectually to this work.

COMPETING FINANCIAL INTERESTS

The authors declare that they have no competing financial interests.

Published online at http://www.nature.com/naturecellbiology/
Reprints and permissions information is available online at http://npg.nature.com/reprintsandpermissions/

1. Bekker-Jensen, S. *et al.* Spatial organization of the mammalian genome surveillance machinery in response to DNA strand breaks. *J. Cell Biol.* **173,** 195–206 (2006).
2. Stucki, M. & Jackson, S. P. γH2AX and MDC1: anchoring the DNA-damage-response machinery to broken chromosomes. *DNA Repair* **5,** 534–543 (2006).
3. Kastan, M. B. & Bartek, J. Cell-cycle checkpoints and cancer. *Nature* **432,** 316–323 (2004).
4. Zhou, B. B. & Elledge, S. J. The DNA damage response: putting checkpoints in perspective. *Nature* **408,** 433–439 (2000).
5. Zou, L. & Elledge, S. J. Sensing DNA damage through ATRIP recognition of RPA-ssDNA complexes. *Science* **300,** 1542–1548 (2003).
6. Shiloh, Y. ATM and related protein kinases: safeguarding genome integrity. *Nature Rev. Cancer* **3,** 155–168 (2003).
7. Kennedy, R. D. & D'Andrea, A. D. The Fanconi Anemia/BRCA pathway: new faces in the crowd. *Genes Dev.* **19,** 2925–2940 (2005).
8. Antoch, M. P., Kondratov, R. V. & Takahashi, J. S. Circadian clock genes as modulators of sensitivity to genotoxic stress. *Cell Cycle* **4,** 901–907 (2005).
9. Fu, L., Pelicano, H., Liu, J., Huang, P. & Lee, C. The circadian gene *Period2* plays an important role in tumor suppression and DNA damage response in vivo. *Cell* **111,** 41–50 (2002).
10. Gery, S. *et al.* The circadian gene *per1* plays an important role in cell growth and DNA damage control in human cancer cells. *Mol. Cell* **22,** 375–382 (2006).
11. Pregueiro, A. M., Liu, Q., Baker, C. L., Dunlap, J. C. & Loros, J. J. The *Neurospora* checkpoint kinase 2: a regulatory link between the circadian and cell cycles. *Science* **313,** 644–649 (2006).
12. Ahmed, S., Alpi, A., Hengartner, M. O. & Gartner, A. *C. elegans* RAD-5/CLK-2 defines a new DNA damage checkpoint protein. *Curr. Biol.* **11,** 1934–1944 (2001).
13. Garcia-Muse, T. & Boulton, S. J. Distinct modes of ATR activation after replication stress and DNA double-strand breaks in *Caenorhabditis elegans*. *EMBO J.* **24,** 4345–4355 (2005).
14. Early, A., Drury, L. S. & Diffley, J. F. Mechanisms involved in regulating DNA replication origins during the cell cycle and in response to DNA damage. *Philos. Trans. R. Soc. Lond. B Biol. Sci.* **359,** 31–38 (2004).
15. Polanowska, J., Martin, J. S., Garcia-Muse, T., Petalcorin, M. I. & Boulton, S. J. A conserved pathway to activate BRCA1-dependent ubiquitylation at DNA damage sites. *EMBO J.* **25,** 2178–2188 (2006).
16. Brown, E. J. & Baltimore, D. ATR disruption leads to chromosomal fragmentation and early embryonic lethality. *Genes Dev.* **14,** 397–402 (2000).
17. Kim, J. E., McAvoy, S. A., Smith, D. I. & Chen, J. Human TopBP1 ensures genome integrity during normal S phase. *Mol. Cell Biol.* **25,** 10907–10915 (2005).
18. Syljuasen, R. G. *et al.* Inhibition of human Chk1 causes increased initiation of DNA replication, phosphorylation of ATR targets, and DNA breakage. *Mol. Cell Biol.* **25,** 3553–3562 (2005).
19. Jaspers, N. G. & Zdzienicka, M. Z. Inhibition of DNA synthesis by ionizing radiation: a marker for an S-phase checkpoint. *Methods Mol. Biol.* **314,** 51–59 (2006).
20. Brown, E. J. & Baltimore, D. Essential and dispensable roles of ATR in cell cycle arrest and genome maintenance. *Genes Dev.* **17,** 615–628 (2003).
21. Chini, C. C. & Chen, J. Human claspin is required for replication checkpoint control. *J. Biol. Chem.* **278,** 30057–30062 (2003).
22. Goldberg, M. *et al.* MDC1 is required for the intra-S-phase DNA damage checkpoint. *Nature* **421,** 952–956 (2003).
23. Lou, Z., Minter-Dykhouse, K., Wu, X. & Chen, J. MDC1 is coupled to activated CHK2 in mammalian DNA damage response pathways. *Nature* **421,** 957–961 (2003).
24. Stewart, G. S., Wang, B., Bignell, C. R., Taylor, A. M. & Elledge, S. J. MDC1 is a mediator of the mammalian DNA damage checkpoint. *Nature* **421,** 961–966 (2003).
25. Xu, B., Kim, S. & Kastan, M. B. Involvement of Brca1 in S-phase and G(2)-phase checkpoints after ionizing irradiation. *Mol. Cell Biol.* **21,** 3445–3450 (2001).
26. Liu, Q. *et al.* Chk1 is an essential kinase that is regulated by Atr and required for the G(2)/M DNA damage checkpoint. *Genes Dev.* **14,** 1448–1459 (2000).
27. Lam, M. H., Liu, Q., Elledge, S. J. & Rosen, J. M. Chk1 is haploinsufficient for multiple functions critical to tumor suppression. *Cancer Cell* **6,** 45–59 (2004).
28. Takai, H. *et al.* Aberrant cell cycle checkpoint function and early embryonic death in *Chk1*$^{-/-}$ mice. *Genes Dev.* **14,** 1439–1447 (2000).
29. Andreassen, P. R., D'Andrea, A. D. & Taniguchi, T. ATR couples FANCD2 monoubiquitination to the DNA-damage response. *Genes Dev.* **18,** 1958–1963 (2004).
30. Stiff, T. *et al.* Nbs1 is required for ATR-dependent phosphorylation events. *EMBO J.* **24,** 199–208 (2005).
31. Wang, X. *et al.* Chk1 mediated phosphorylation of FANCE is required for the Fanconi Anemia/BRCA pathway. *Mol. Cell Biol.* doi: 10.1128/MCB.02357-06 (2007).
32. Garcia-Higuera, I. *et al.* Interaction of the Fanconi anemia proteins and BRCA1 in a common pathway. *Mol. Cell* **7,** 249–262 (2001).
33. Collis, S. J., Barber, L. J., Ward, J. D., Martin, J. S. & Boulton, S. J. *C. elegans* FANCD2 responds to replication stress and functions in interstrand cross-link repair. *DNA Repair* **5,** 1398–1406 (2006).
34. Sorensen, C. S. *et al.* The cell-cycle checkpoint kinase Chk1 is required for mammalian homologous recombination repair. *Nature Cell Biol.* **7,** 195–201 (2005).
35. Johnson, R. D. & Jasin, M. Double-strand-break-induced homologous recombination in mammalian cells. *Biochem. Soc. Trans.* **29,** 196–201 (2001).
36. Saleh-Gohari, N. *et al.* Spontaneous homologous recombination is induced by collapsed replication forks that are caused by endogenous DNA single-strand breaks. *Mol. Cell Biol.* **25,** 7158–7169 (2005).
37. Zhao, H. & Piwnica-Worms, H. ATR-mediated checkpoint pathways regulate phosphorylation and activation of human Chk1. *Mol. Cell Biol.* **21,** 4129–4139 (2001).
38. Bartek, J., Lukas, C. & Lukas, J. Checking on DNA damage in S phase. *Nature Rev. Mol. Cell Biol.* **5,** 792–804 (2004).
39. Chini, C. C., Wood, J. & Chen, J. Chk1 is required to maintain Claspin stability. *Oncogene* **25,** 4165–4171 (2006).
40. Kumagai, A. & Dunphy, W. G. Claspin, a novel protein required for the activation of Chk1 during a DNA replication checkpoint response in *Xenopus* egg extracts. *Mol. Cell* **6,** 839–849 (2000).
41. Rao, V. A. *et al.* Phosphorylation of BLM, dissociation from topoisomerase IIIα, and colocalization with γ-H2AX after topoisomerase I-induced replication damage. *Mol. Cell Biol.* **25,** 8925–8937 (2005).
42. Zhang, Y. W. *et al.* Genotoxic stress targets human Chk1 for degradation by the ubiquitin-proteasome pathway. *Mol. Cell* **19,** 607–618 (2005).
43. Tercero, J. A. & Diffley, J. F. Regulation of DNA replication fork progression through damaged DNA by the Mec1/Rad53 checkpoint. *Nature* **412,** 553–557 (2001).
44. Howlett, N. G., Taniguchi, T., Durkin, S. G., D'Andrea, A. D. & Glover, T. W. The Fanconi anemia pathway is required for the DNA replication stress response and for the regulation of common fragile site stability. *Hum. Mol. Genet.* **14,** 693–701 (2005).
45. O'Driscoll, M., Ruiz-Perez, V. L., Woods, C. G., Jeggo, P. A. & Goodship, J. A. A splicing mutation affecting expression of ataxia-telangiectasia and Rad3-related protein (ATR) results in Seckel syndrome. *Nature Genet.* **33,** 497–501 (2003).
46. Dimitrova, D. S. & Gilbert, D. M. Temporally coordinated assembly and disassembly of replication factories in the absence of DNA synthesis. *Nature Cell Biol.* **2,** 686–694 (2000).
47. Feijoo, C. *et al.* Activation of mammalian Chk1 during DNA replication arrest: a role for Chk1 in the intra-S phase checkpoint monitoring replication origin firing. *J. Cell Biol.* **154,** 913–923 (2001).
48. Jiang, N., Benard, C. Y., Kebir, H., Shoubridge, E. A. & Hekimi, S. Human CLK2 links cell cycle progression, apoptosis, and telomere length regulation. *J. Biol. Chem.* **278,** 21678–21684 (2003).

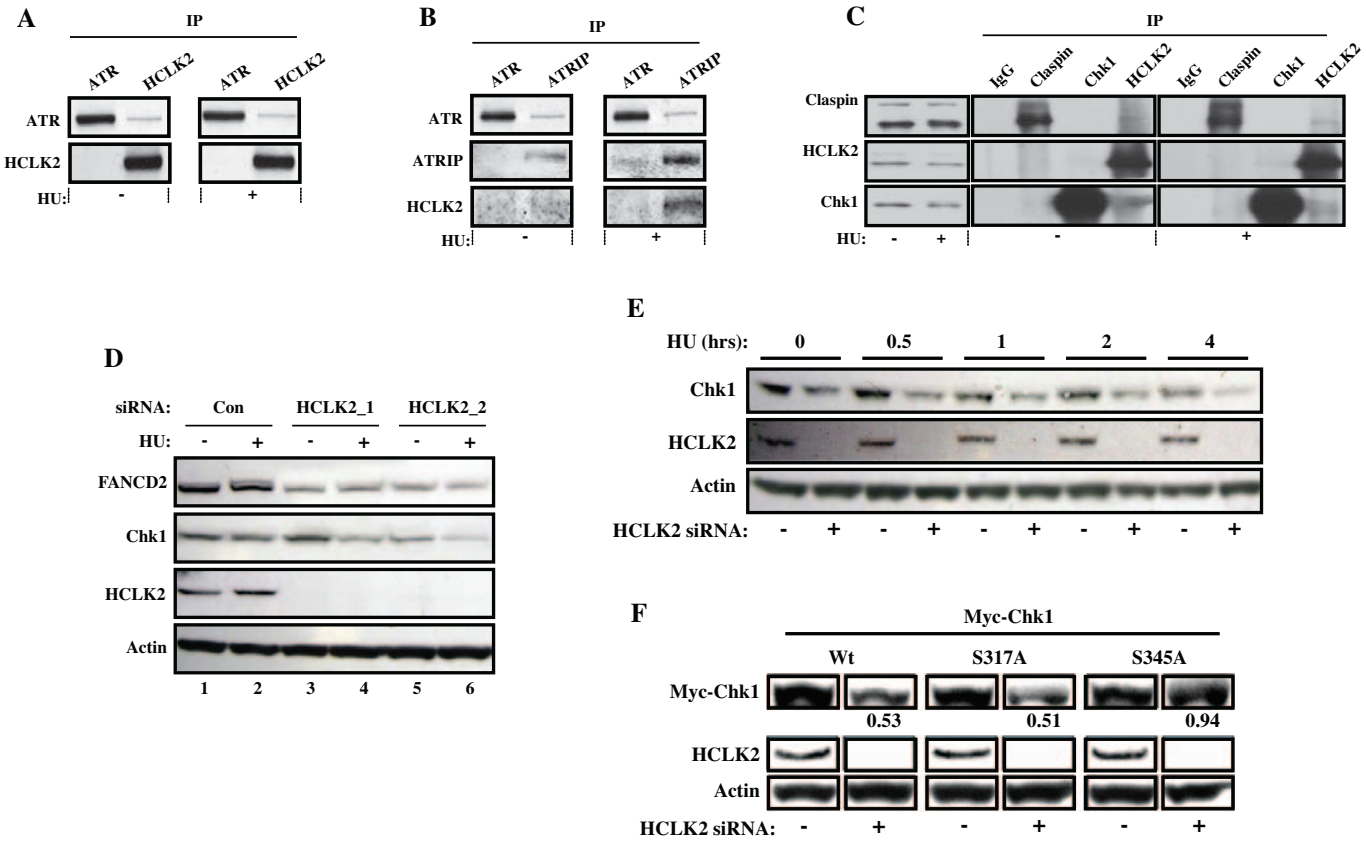

Figure S1 HCLK2 associates with ATR, ATRIP, Chk1 and Claspin and impacts on Chk1 stability. **A.** Western blotting for ATR and HCLK2 following immunoprecipitation for ATR and HLCK2 from untreated or HU (3mM, 2hrs) treated HeLa cells. **B.** Western blotting for ATR, ATRIP and HCLK2 following immunoprecipitation for ATR and ATRIP from untreated or HU (3mM, 2hrs) treated HeLa cells. **C.** Western blotting for Claspin, HCLK2 and Chk1 following immunoprecipitation for Claspin, HCLK2 and Chk1 from untreated or HU (3mM, 2hours) treated HeLa cell extracts. **D**. Western blotting with the indicated antibodies of extracts derived from cells treated with control (-) and two single HCLK2 (+) siRNAs (HCLK2_1 and HCLK2_2) before and 2 hours after treatment with 3 mM HU **E**. Western blotting with the indicated antibodies of extracts derived from control (-) and HCLK2 (+) siRNA treated cells before and at the indicated time points after treatment with 3 mM HU. **F.** Western blotting for transfected Myc-Chk1, HCLK2 and actin following transfection with Myc-Chk1 wild type, S317A, or S345A alleles, 48 hours after control or HCLK2 siRNA treatments. The indicated levels of Myc-Chk1 were quantified using Biorad geldoc quantity-one software, and are expressed relative to the levels in control cells.

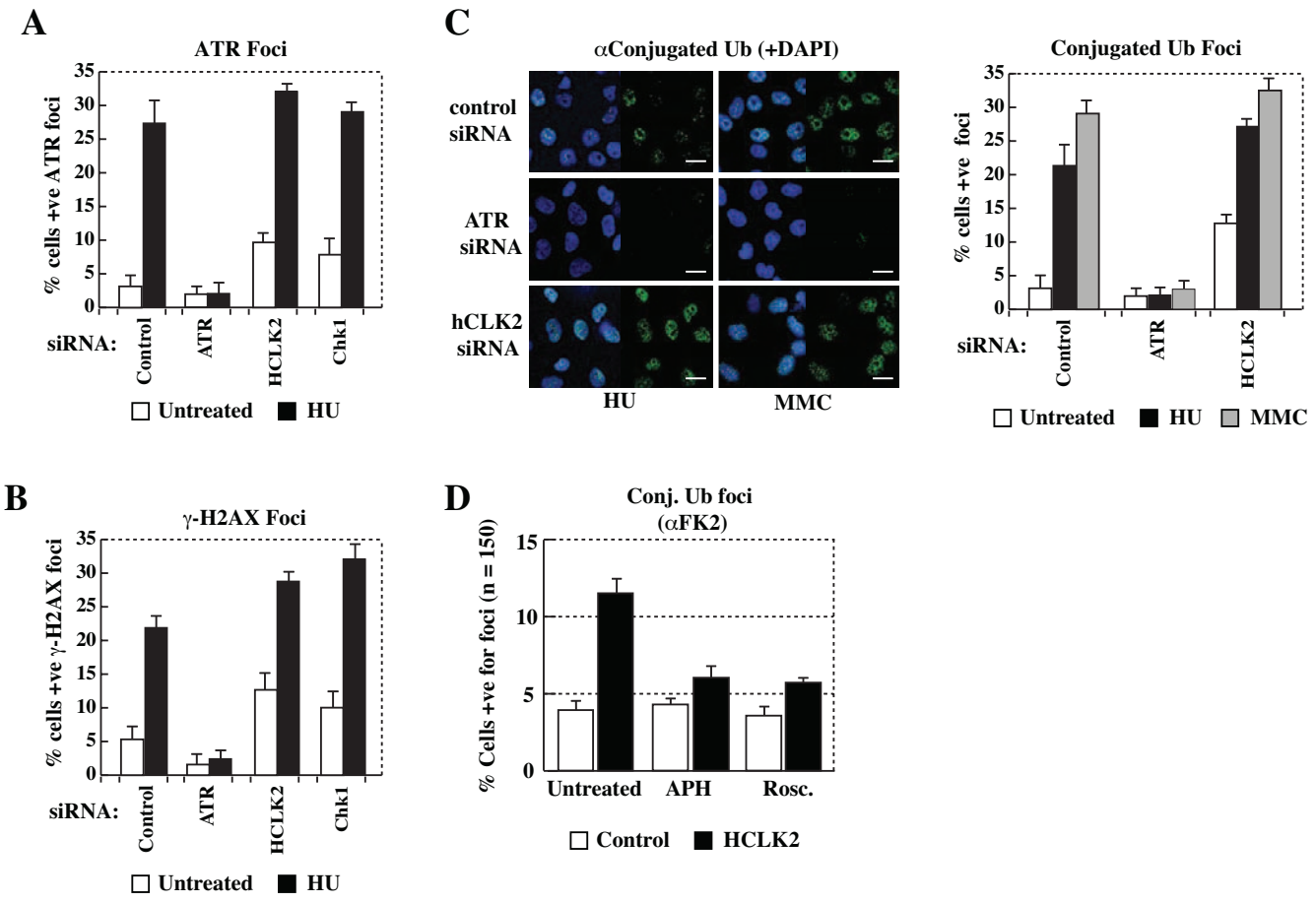

Figure S2 HCLK2 deficiency increases a subset of ATR-dependent S-phase checkpoint responses following replication stress **A.** Quantification of the number of cells positive for ATR foci in untreated (white bars) or 3 mM HU (2 h) treated cells (black bars), after transfection of control, ATR, HCLK2 and Chk1 siRNAs. Error bars indicate s.e.m. from 3 separate experiments. **B.** Quantification of the number of cells positive for γ-H2AX foci in untreated (white bars) or 3 mM HU (2 h) treated cells (black bars), after transfection of control, ATR, HCLK2 and Chk1 siRNAs. Error bars indicate s.e.m. from 3 separate experiments. **C.** Representative images of conjugated Ub (FK2) immuno-staining in 3mM HU (2 h) or 80 ng/ml MMC (18 h) treated HeLa cells after transfection of control, ATR, or HCLK2 siRNAs. The corresponding quantifications of foci-positive cells are shown in the graph below, with error bars indicating s.e.m. from 3 separate experiments. **D.** Quantification of the number of cells positive for conjugated Ub foci in untreated, aphidicolin (10μM) and roscovitine (10 μg/ml) treated cells, after transfection of control or HCLK2 siRNAs. Drugs were added 4 hours prior to fixation.

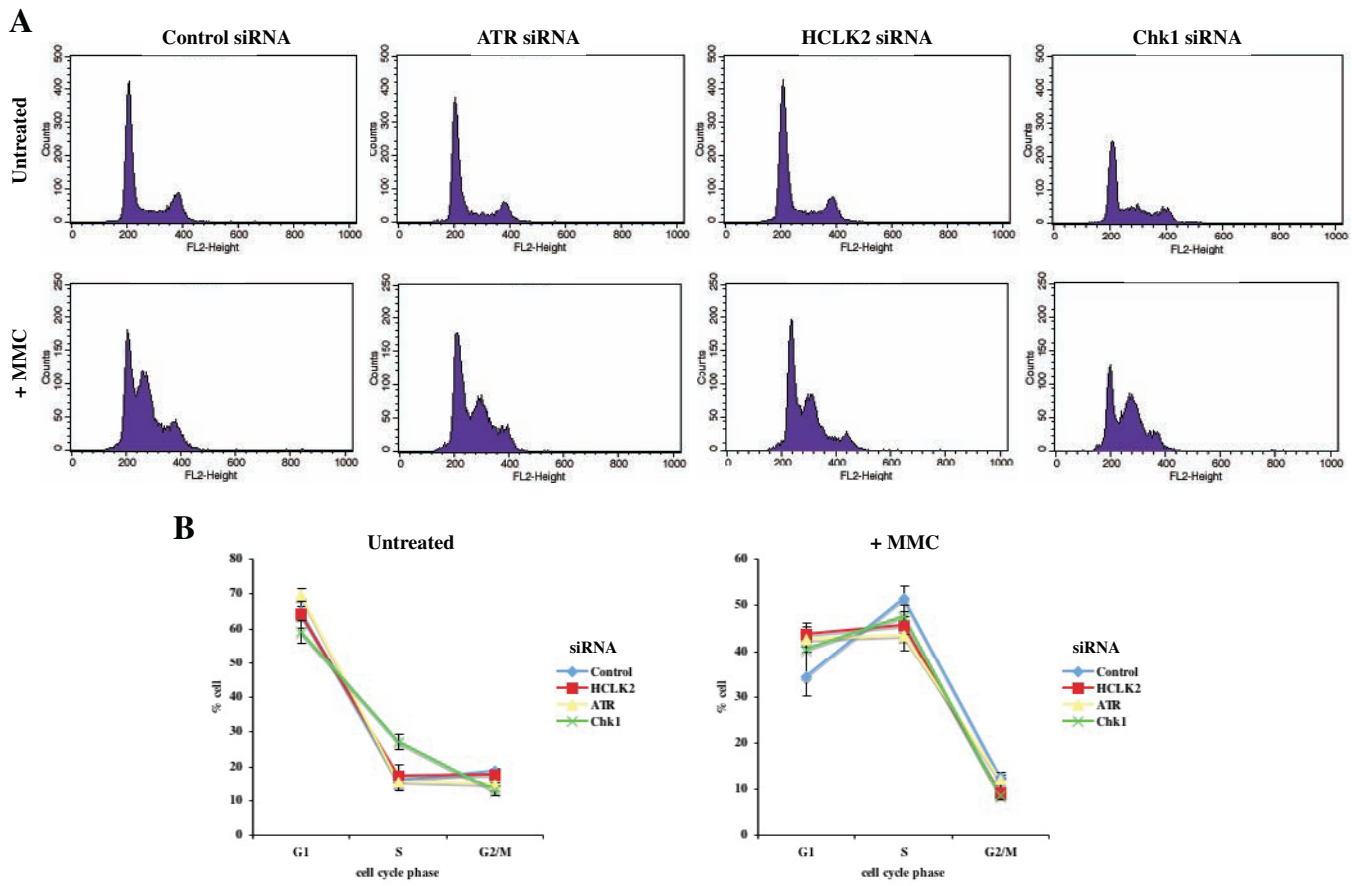

Figure S3 Cell cycle analysis of ATR, HCLK2 and Chk1 siRNA treated cells before and after MMC treatment. **A.** Representative cell cycle profiles of asynchronous HeLa cells 72 hours post transfection with control, ATR, HCLK2 and Chk1 siRNA for untreated and 80ng/ml MMC (treated after 60 hours for 12 hours). **B**. Percentage of cells in G1, S and G2/M stages of the cell cycle subjected to the indicated siRNA treatments (as in A) either left untreated or treated with 80ng/ml MMC (treated after 60 hours for 12 hours). Error bars indicate s.e.m. from 4 independent experiments.

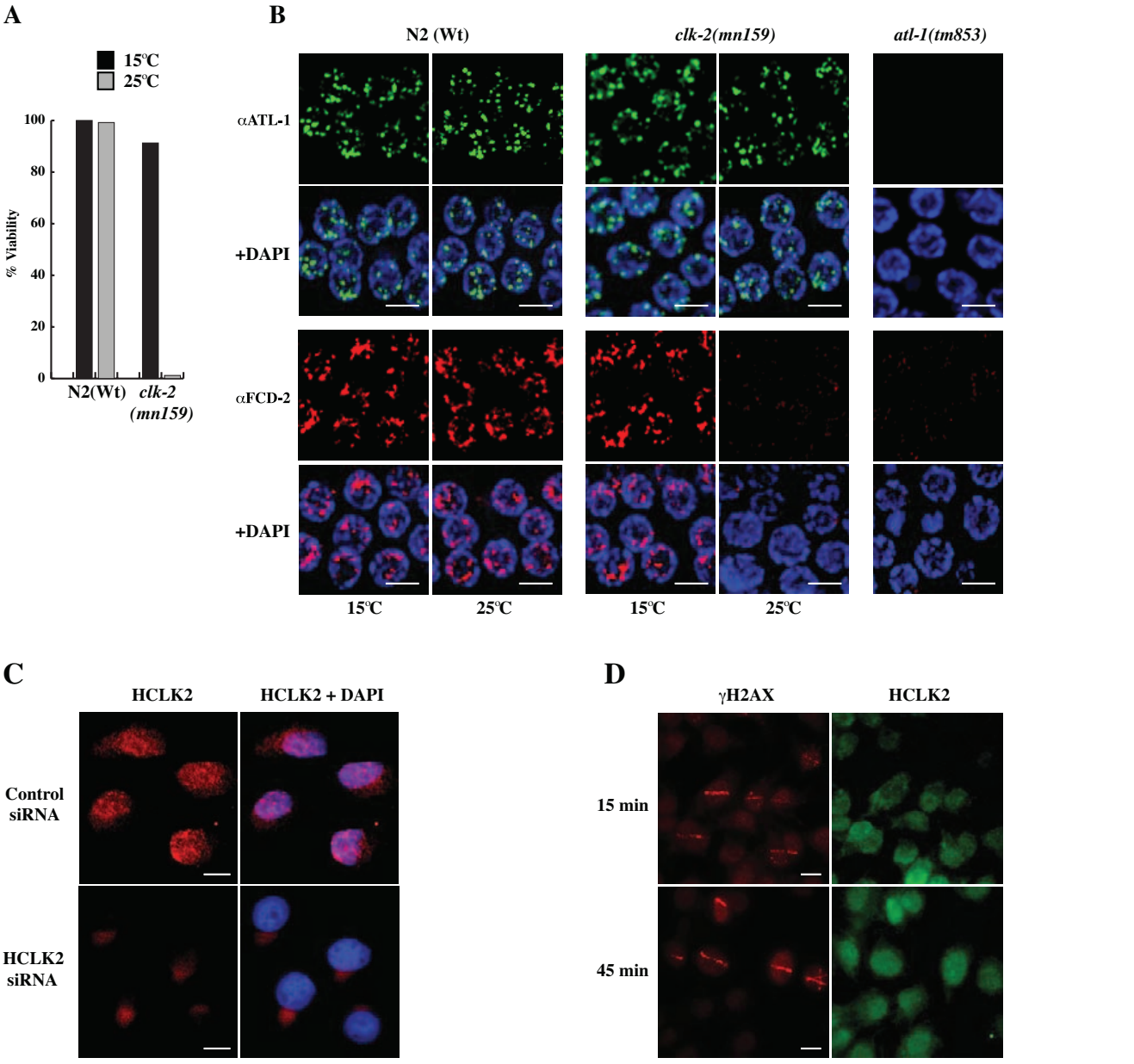

Figure S4 ATL-1 and FCD-2 focus formation in *clk-2(mn159)* mutants at its permissive and non-permissive temperatures. **A**. Shown is the % viability of N2(Wt) and *clk-2(mn159)* strains at 15°C (Black) and 25°C (Grey) (permissive and non-permissive for *clk-2(mn159)*, respectively). *clk-2(qm37)* is also viable at 15°C and inviable at 25°C (data not shown). **B**. Representative images of ATL-1 and FCD-2 immuno-staining in the mitotic region of the germline 18 hours post treatment with 180 μM Cisplatin (CDDP) in animals of the indicated genotype. N2(Wt) and *clk-2(mn159)* strains were grown and treated at the indicated temperatures. *atl-(tm853)* mutants are defective for ATL-1 and FCD-2 at both 15°C and 25°C (data not shown). It should be noted that biological clock function of CLK-2 is compromised in *clk-2(mn159)* and *clk-2(qm37)* mutants at 15°C[1], although the checkpoint remains intact until the temperature is shifted to 20°C[12]. This would suggest that the biological clock and checkpoint functions of CLK-2 are separable. HCLK2 is a nuclear protein that is not detectably retained at sites of laser-induced DNA damage. **C**. Representative images of untreated HeLa cells transfected with control or HCLK2 siRNA and then fixed and immunostained with antibodies specific to HCLK2 and counter-stained with DAPI. The nuclear staining observed with HCLK2 antibodies is eliminated by HCLK2 siRNA, but not by control siRNA. A similar diffuse nuclear pattern of HCLK2 protein was observed with two independently derived antibodies (data not shown). **D**. HeLa cells were microirradiated and then co-immunostained with antibodies to γ-H2AX and HCLK2 at the indicated times post treatment. γ-H2AX is rapidly induced at sites of laser-induced DNA damage. No detectable retention of HCLK2 at sites of laser-induced DNA damage was observed at 15 or 40 minutes post treatment. No discernable retention of HCLK2 in foci was observed 120 minutes post microirradiation or following 3mM HU or 80 ng/ml MMC treatment (data not shown).

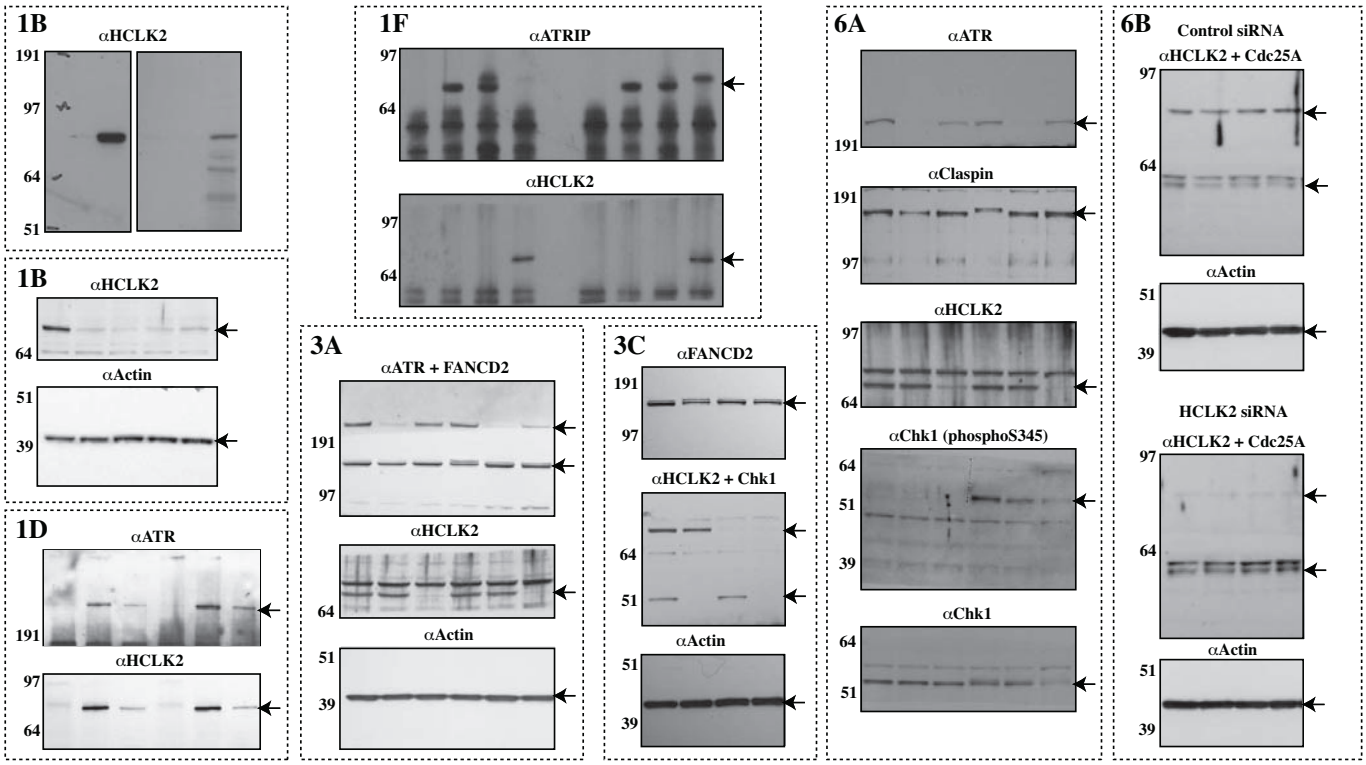

Figure S5 Expanded blots including molecular weight size markers from the indicated selected figures.

REFERENCES

Lakowski, B. & Hekimi, S. Determination of life-span in *Caenorhabditis elegans* by four clock genes. *Science* **272**, 1010–1013 (1996).